# On-shell renormalisation constants including two different nonzero masses

S. Bekavac, D. Seidel

Institut für Theoretische Teilchenphysik, Universität Karlsruhe (TH)
76128 Karlsruhe, Germany

We present results for the effect of a second massive quark in the relation between the pole and the minimal subtracted quark mass at the three loop level. We also consider the analogous effect for the wave function renormalisation constant. Some technical details of the calculation are given. Our result is phenomenologically relevant for the bottom quark including virtual charm effects.

## 1 Introduction

Quark masses are fundamental parameters of the Standard Model (SM) and thus it is desirable to determine their numerical values with the highest possible precision. In order to do so it is necessary to fix a renormalisation scheme which defines the quark mass. Often physical observables are expressed through some "short distance" mass [1] to obtain predictions which are free of the renormalon problem. To do so, one frequently needs the relation between the on-shell and the $\overline{\mathrm{MS}}$ mass. Many authors contributed to the latter task [2, 3, 4]. In this contribution we present the recently published calculation [5], where we have included the effect of a second nonzero quark mass to the relation between the quarks in those two schemes at the three loop level. After having reduced the problem to the calculation of master integrals we use two different ways to solve them, namely the differential equation and the Mellin-Barnes method. From the phenomenological point of view this result is important for the bottom-quark including effects from virtual charm-quarks. As a byproduct we also obtain the corresponding contribution to the wave function renormalisation constant.

## 2 Renormalisation constants

Introducing the decomposition of the quark self-energy

$$\Sigma(q, m_q) \quad = \quad m_q\, \Sigma_1(q^2, m_q) + (\not{q} - m_q)\, \Sigma_2(q^2, m_q)\,, \tag{1}$$

we can express the renormalisation constants, which are defined through

$$m_{q,0} = Z_m^{\mathrm{OS}}\, M_q\,, \qquad \psi_0 = \sqrt{Z_2^{\mathrm{OS}}}\, \psi\,, \tag{2}$$

by [6, 4]

$$\begin{aligned} Z_m^{\mathrm{OS}} \quad &= \quad 1 + \Sigma_1(M_q^2, M_q)\,, && (3) \\ \left(Z_2^{\mathrm{OS}}\right)^{-1} \quad &= \quad 1 + 2M_q^2 \frac{\partial}{\partial q^2} \Sigma_1(q^2, M_q)\Big|_{q^2 = M_q^2} + \Sigma_2(M_q^2, M_q)\,. && (4) \end{aligned}$$

$\psi$ is the quark field renormalised in the on-shell scheme with mass $m_q$, $M_q$ is the on-shell mass and bare quantities are denoted by a subscript 0. Thus, to obtain $Z_m^{\mathrm{OS}}$ one only needs

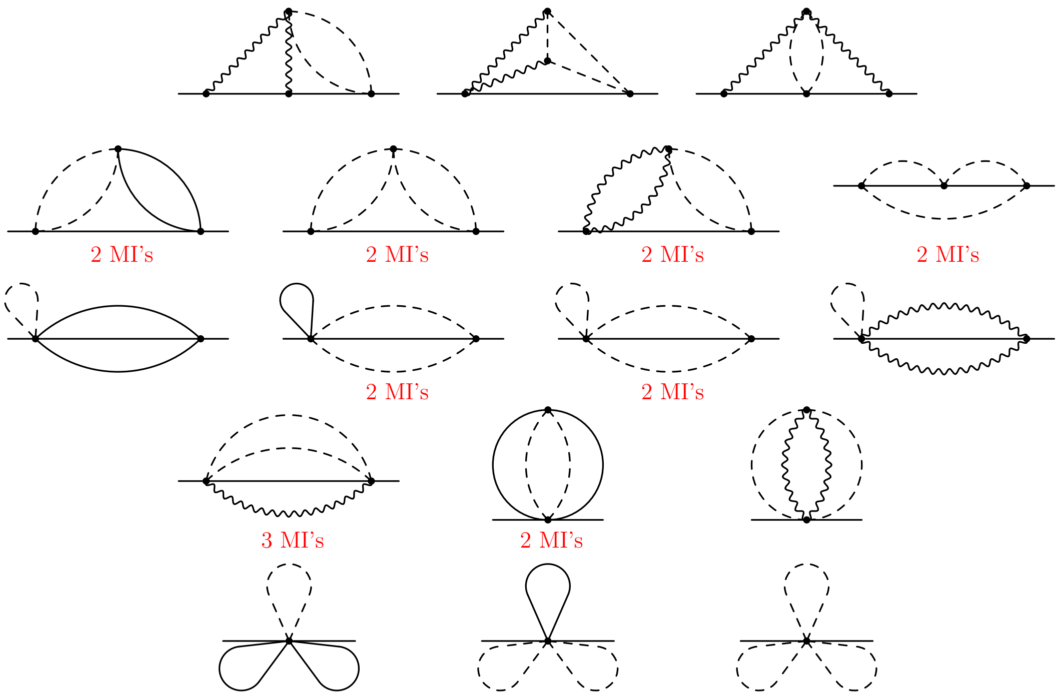


Figure 1: Master integrals. The solid/wavy lines correspond to particles with mass $M_q/0$, the dashed lines denote the quark with the second nonzero mass.

to calculate $\Sigma_1$ for $q^2 = M_q^2$. To calculate $Z_2^{\rm OS}$, one has to compute the first derivative of the self-energy diagrams. The mass renormalisation is taken into account iteratively by calculating one- and two-loop diagrams with zero-momentum insertions.

In the case of the mass renormalisation it is convenient to consider the ratio between the on-shell and $\overline{\rm MS}$ renormalisation constants

$$z_m \quad = \quad \frac{Z_m^{\rm OS}}{Z_m^{\overline{\rm MS}}} \quad = \quad \frac{m_q(\mu)}{M_q} \tag{5}$$

which is finite. Here we have introduced the renormalisation dependent $\overline{\rm MS}$-mass $m_q(\mu)$.

In contrast to $Z_m^{\rm OS}$ the wave function renormalisation constant contains next to ultraviolet also infrared divergences. Thus it is not possible to construct a finite quantity by considering the ratio between the on-shell and $\overline{\rm MS}$ renormalisation constant.

## 3 Computational techniques

In order to compute the on shell self energy we use `QGRAF` [7] to generate the feynman diagrams and the various topologies are identified with the help of `q2e` and `exp` [8, 9]. In a next step the reduction of the various functions to so-called master integrals (MI's) has to be achieved. For this step we use the so-called Laporta method [10, 11] which reduces the three-loop integrals to 26 MI's. We use the implementation of Laporta's algorithm in the program `Crusher` [12]. It is written in `C++` and uses `GiNaC` [13] for simple manipulations like taking derivatives of polynomial quantities. In the practical implementation of the Laporta algorithm one of the most time-consuming operations is the simplification of the coefficients appearing in front of the individual integrals. This task is performed with the help of `Fermat` [14] where a special interface has been used (see Ref. [15]). The main features of the implementation are the automated generation of the integration-by-parts (IBP) identities [16], a complete symmetrisation of the diagrams and the possibility to use multiprocessor environments.

In Fig. 1 a graphical representation of the master integrals can be found. As indicated in the figure, many topologies contain more than one master integral. We have chosen two independent ways to compute the $\varepsilon$-expansion of the master integrals. The first one relies on the differential equation method [17]. With this method we were able to evaluate all but four master integrals in analytic form. With the help of our second method, based on the Mellin-Barnes technique (see, e.g., Ref. [18]) we can get numerical results for all master integrals. Here we have used the `Mathematica` package `MB.m` [19].

### 3.1 Differential-Equation-Method

First we set up differential equations in $z = M_f/M_q$, where $M_f$ is the second nonzero quark mass, for each of the individual integrals. Each equation will contain the master integral itself and integrals belonging to the corresponding topology. The latter can again be reduced to the set of master integrals. For all the topologies which contain only one master integral (e.g. all six-propagator integrals in Fig. 1) this gives a "simple" equation whereas for the other topologies we get two or three coupled equations, respectively. In the next step we expand the differential equations in $\varepsilon$. Choosing an appropriate basis for the master integrals, all equations decouple order by order in $\varepsilon$. We can now solve for all integrals by repeated use of Euler's variation of the constant method. The initial conditions we need are all known from the literature [20, 21, 22, 6].

We were able to get analytical results for all master integrals in terms of Harmonic Polylogarithms (HPL's [23]) up to order $\varepsilon^{-1}$. Unfortunately we were not yet able to get analytical results in higher orders in $\varepsilon$ for the four integrals belonging to the two topologies depicted as the leftmost ones in the second row of Fig. 1. For all other integrals we provide analytical results up to the order we need in our calculation. To calculate the MI's in terms of HPL's it is necessary that the (pseudo)poles in the corresponding differential equations are all of the form $1/z$, $1/(z+1)$ and $1/(z-1)$, were these poles can occur up to arbitrary order. This is the case in all topologies except for the ones mentioned above. We have not found a proper change of variables to bring the differential equation into this form. As a consequence we only managed to integrate the integrals in these topologies up to the order $\varepsilon^{-1}$. The remaining parts can e.g. be integrated numerically with Mathematica.

To evaluate our results numerically and for general algebraic manipulations of terms involving HPL's we use the Mathematica package HPL [24, 25].

### 3.2 Mellin-Barnes-Method

The Mellin-Barnes method as a tool for the evaluation of Feynman integrals has become very popular in the recent years. The basic formula is [18]

$$\frac{1}{(X+Y)^{\lambda}} = \frac{1}{\Gamma(\lambda)} \frac{1}{2\pi i} \int_{-i\infty}^{i\infty} dz\, \Gamma(1+z)\Gamma(-z) \frac{Y^z}{X^{\lambda+z}}, \tag{6}$$

which transforms a propagator like term into a complex contour integral. A common recipe to evaluate Feynman integrals is the following: First one introduces Feynman parameters for a loop variable. Then one can perform the corresponding momentum integration. After that one applies formula (6) to the denominators containing the Feynman parameters. Finally the Feynman parameters can be integrated yielding the Mellin-Barnes representation of the original integral. This procedure has recently been automatised [26].

The Mellin-Barnes integration is to be performed along a contour which reaches from $-\infty$ to $\infty$ on the imaginary axis with indentations such that the poles of $\Gamma(\ldots + z)$ and those of $\Gamma(\ldots - z)$ are separated by the contour.

Mellin-Barnes integrals usually have singularities for certain values of their parameters. If there are for example Gamma functions of the form $\Gamma(\varepsilon + z)\,\Gamma(-z)$, it is not possible to find an appropriate integration contour when $\varepsilon \to 0$. The integral is therefore singular in $\varepsilon$ and this is how UV poles of Feynman integrals manifest themselves in their Mellin-Barnes representation. One has thus to regularise the integral, that is, identify the $\varepsilon$ poles. This can be done by shifting the integration contour using the residue theorem. Prescriptions to do so have been given in Refs. [27] and [28], the latter has been automatised, see Refs. [29, 19].

Finally the regularised integrals can be expanded in $\varepsilon$ and evaluated by numerical integration, which is also implemented in the package `MB.m` [19], or by application of the residue theorem and summing up the residues. Depending on the dimension of the integrals and the complexity of the integrand this can be done numerically or analytically.

To calculate the master integrals for this work we first simplified the Mellin-Barnes integrals by inserting the representations of known subtopologies. The regularisation has been done partly using `MB.m` and the approach of Ref. [27]. One- and two-dimensional MB-integrals were calculated via their sum representation, higher dimensional integrals using `MB.m`.

The 4-line integrals can all be represented as Mellin-Barnes-integrals of maximal dimension 1, which can be evaluated as single sums. For the 5 line master integrals we find representations of dimension 2 to 5. The integrals with 6 lines have 3 to 5 dimensional representations. We find good agreement with the results obtained from the differential equation method.

Inserting the results for the master integrals into the final result we observe large numerical cancellations near $M_f = 0$ between the contributions originating from different master integrals. On the other hand, the expansion for $M_f/M_q \ll 1$ converges very fast, which is relevant for $M_f = m_c$ and $M_q = m_b$. For this reason we decided to derive an expansion of our result including eighth order terms. The coefficients that could not be obtained analytically can be evaluated numerically from their Mellin-Barnes-representation, which is in our case at most two-dimensional.

## 4 Results and applications

As an application of our result we want to discuss the charm quark effects in the relations between the pole, the $\overline{\rm MS}$ and the $1S$ quark mass. For illustration we use $m_b(m_b) = 4.2$ GeV, $m_c(m_c) = 1.3$ GeV, $\mu = m_b$ and $\alpha_s^{(4)}(m_b) = 0.2247$. The relation between the on-shell and the $\overline{\rm MS}$ mass leads to

$$M_b = \left[4.2 + 0.401 + \left(0.199 + 0.0094\Big|_{m_c}\right) + \left(0.145 + 0.0182\Big|_{m_c}\right)\right] \text{GeV}\,, \qquad (7)$$

where the tree-level, one-, two- and three-loop results are shown separately. The contributions from the charm quark mass which vanish for $m_c \to 0$ are marked by a subscript $m_c$. One observes that the higher order contributions are significant. In particular, the two-loop charm quark effects amount to 9 MeV and the three-loop ones to 18 MeV. A similar bad convergence is observed in the relation between the $1S$ mass [30] $M_b^{1S}$ and the pole mass $M_b$. For $M_b = 4.8$ GeV, $m_c(m_c) = 1.3$ GeV, $\mu = M_b$ and $\alpha_s^{(4)}(M_b) = 0.2150$ it is given by

$$M_b^{1S} = \left[4.8 - 0.049 - \left(0.073 + 0.0041\Big|_{m_c}\right) - \left(0.098 + 0.0112\Big|_{m_c}\right)\right] \text{GeV}\,. \qquad (8)$$

However, the relation between the $1S$ and the $\overline{\rm MS}$ quark mass is much better behaved as can be seen in the following example where we have chosen $M_b^{1S} = 4.69$ GeV, $m_c(m_c) = 1.3$ GeV, $\mu = M_b^{1S}$ and $\alpha_s^{(4)}(M_b^{1S}) = 0.2167$

$$m_b = \left[4.69 - 0.382 - \left(0.098 + 0.0047\Big|_{m_c}\right) - \left(0.030 + 0.0051\Big|_{m_c}\right)\right] \text{GeV}\,. \qquad (9)$$

The two-loop charm effects amount to only 4.7 MeV and three-loop ones to 5.1 MeV. We want to mention that in case only the linear approximation [3] of the charm quark mass effects is used the corresponding three-loop results in Eqs. (7) and (9) read 0.0167 and 0.0037, respectively.

## Acknowledgements

We would like to thank Andrey Grozin and Matthias Steinhauser for a fruitful collaboration on this subject. This work was supported the DFG through SFB/TR 9.

## References

[1] M. Beneke, Phys. Lett. B **434** (1998) 115 [arXiv:hep-ph/9804241]. K. Melnikov and A. Yelkhovsky, Phys. Rev. D **59** (1999) 114009 [arXiv:hep-ph/9805270]. A. H. Hoang, Phys. Rev. D **61** (2000) 034005 [arXiv:hep-ph/9905550].

[2] R. Tarrach, Nucl. Phys. B **183** (1981) 384. N. Gray, D. J. Broadhurst, W. Grafe and K. Schilcher, Z. Phys. C **48** (1990) 673. D. J. Broadhurst, N. Gray and K. Schilcher, Z. Phys. C **52** (1991) 111. K. G. Chetyrkin and M. Steinhauser, Phys. Rev. Lett. **83** (1999) 4001 [arXiv:hep-ph/9907509]. K. G. Chetyrkin and M. Steinhauser, Nucl. Phys. B **573** (2000) 617 [arXiv:hep-ph/9911434]. K. Melnikov and T. van Ritbergen, Phys. Lett. B **482** (2000) 99 [arXiv:hep-ph/9912391]. K. Melnikov and T. van Ritbergen, Nucl. Phys. B **591** (2000) 515 [arXiv:hep-ph/0005131].

[3] A. H. Hoang, arXiv:hep-ph/0008102.

[4] P. Marquard, L. Mihaila, J. H. Piclum and M. Steinhauser, Nucl. Phys. B **773** (2007) 1 [arXiv:hep-ph/0702185].

[5] S. Bekavac, A. Grozin, D. Seidel and M. Steinhauser, arXiv:0708.1729 [hep-ph].

[6] K. Melnikov and T. van Ritbergen, Nucl. Phys. B **591** (2000) 515 [arXiv:hep-ph/0005131].

[7] P. Nogueira, J. Comput. Phys. **105** (1993) 279.

[8] R. Harlander, T. Seidensticker and M. Steinhauser, Phys. Lett. B **426** (1998) 125 [hep-ph/9712228].

[9] T. Seidensticker, hep-ph/9905298.

[10] S. Laporta and E. Remiddi, Phys. Lett. B **379** (1996) 283 [arXiv:hep-ph/9602417].

[11] S. Laporta, Int. J. Mod. Phys. A **15** (2000) 5087 [arXiv:hep-ph/0102033].

[12] P. Marquard and D. Seidel, unpublished.

[13] C. Bauer, A. Frink and R. Kreckel, arXiv:cs.sc/0004015.

[14] R. H. Lewis, Fermat's User Guide, http://www.bway.net/~lewis.

[15] M. Tentyukov and J. A. M. Vermaseren, arXiv:cs.sc/0604052.

[16] K. G. Chetyrkin and F. V. Tkachov, Nucl. Phys. B **192** (1981) 159.

[17] A. V. Kotikov, Phys. Lett. B **254** (1991) 158.

[18] V. A. Smirnov, Springer Tracts Mod. Phys. **211** (2004) 1.

[19] M. Czakon, Comput. Phys. Commun. **175** (2006) 559 [arXiv:hep-ph/0511200].

[20] M. Argeri, P. Mastrolia and E. Remiddi, Nucl. Phys. B **631**, 388 (2002) [arXiv:hep-ph/0202123].

[21] P. Mastrolia and E. Remiddi, Nucl. Phys. B **657** (2003) 397 [arXiv:hep-ph/0211451].

[22] P. Marquard, J. H. Piclum, D. Seidel and M. Steinhauser, Nucl. Phys. B **758** (2006) 144 [arXiv:hep-ph/0607168].

[23] E. Remiddi and J. A. M. Vermaseren, Int. J. Mod. Phys. A **15** (2000) 725 [arXiv:hep-ph/9905237].

[24] D. Maitre, Comput. Phys. Commun. **174** (2006) 222 [arXiv:hep-ph/0507152].

[25] D. Maitre, arXiv:hep-ph/0703052.

[26] J. Gluza, K. Kajda and T. Riemann, arXiv:0704.2423 [hep-ph].

[27] V. A. Smirnov, Phys. Lett. B **460** (1999) 397 [arXiv:hep-ph/9905323].

[28] J. B. Tausk, Phys. Lett. B **469** (1999) 225 [arXiv:hep-ph/9909506].

[29] C. Anastasiou and A. Daleo, JHEP **0610** (2006) 031 [arXiv:hep-ph/0511176].

[30] A. H. Hoang, M. C. Smith, T. Stelzer and S. Willenbrock, Phys. Rev. D **59** (1999) 114014 [arXiv:hep-ph/9804227].